A sporulation-independent way of life for *Bacillus thuringiensis* in the late stages of an infection

Hasna Toukabri, Didier Lereclus and Leyla Slamti*

Micalis Institute, INRAE, AgroParisTech, Université Paris-Saclay, 78350 Jouy-en-Josas, France

*Corresponding author: leyla.slamti@inrae.fr

The authors declare that there are no competing interests in relation to the work described.

ABSTRACT

The formation of endospores has been considered as the unique mode of survival and transmission of sporulating Firmicutes due to the exceptional resistance and persistence of this bacterial form. However, the persistence of non-sporulated bacteria (Spo^-) was reported during infection in *Bacillus thuringiensis*, an entomopathogenic sporulating Gram-positive bacterium. In this study, we investigated the behavior of a bacterial population in the late stages of an infection as well as the characteristics of the Spo^- bacteria in the *B. thuringiensis*/*Galleria mellonella* infection model. Using fluorescent reporters coupled to flow cytometry as well as molecular markers, we demonstrated that the Spo^- cells constitute about half of the population two weeks post-infection (pi) and that these bacteria present vitality signs. However, a protein synthesis and a growth recovery assay indicated that they are in a metabolically slowed-down state. Interestingly, they were extremely resistant to the cadaver environment which proved deadly for *in vitro*-grown vegetative cells and, strikingly, did not support spore germination. A transcriptomic analysis of this subpopulation at 7 days pi revealed a signature profile of this state. The expression analysis of individual genes at the cell level suggests that iron homeostasis is important at all stages of the infection, whereas the oxidative stress response seems of particular importance as the survival time increases. Altogether, these data show that non-sporulated bacteria are able to survive for a prolonged period of time and indicate that they engage in a profound adaptation process that leads to their persistence in the host cadaver.

INTRODUCTION

The ability of bacteria to face environmental fluctuations is essential to their survival. These stresses include nutrient limitation or depletion, variations of pH, temperature, oxygen level, osmolarity, radiation and chemical exposure. In conditions that do not support their growth, some Firmicutes, such as *Bacillus* species, have evolved the ultimate mode of resistance, sporulation [1]. This survival mode requires the activation of a specific and complex developmental pathway that leads to the formation of a spore, a highly resistant dormant cell that allows these species to survive in extreme conditions during extended periods [2–5]

Due to their resistant nature, the formation of endospores was considered the unique mode of survival and transmission of these sporulating species. However, it was recently shown that a *Bacillus subtilis* sporulation mutant was able to survive deep starvation during several months by entering an oligotrophic state that supports extreme slow growth [6]. Moreover, spontaneous mutants in *spo0A*, the gene specifying the master regulator of sporulation [7,8], were isolated alongside spores after a month-long incubation of the food-borne pathogen *Bacillus cereus* under abiotic conditions in groundwater [9]. Furthermore, a *B. cereus* strain impaired in sporulation was shown to persist for several days on ready-to-eat vegetables and retained its ability to cause illness in a mammalian host [10]. In addition, it was shown that spores represented only 30% of the bacterial population that survived in an insect cadaver 4 days pi (dpi) with *Bacillus thuringiensis* and that a sporulation mutant was able to persist in the cadaver during that time [11].

B. thuringiensis is an entomopathogenic bacterium that belongs to the *B. cereus sensu lato* group comprising several species that are pathogenic to humans and animals, notably *B. cereus sensu stricto*, which is responsible for foodborne toxi-infections as well as systemic infections, and *Bacillus anthracis*, the agent of anthrax [12]. *B. thuringiensis* was shown to carry out a full infectious cycle in the *Galleria mellonella* insect larvae model. This process is composed of

three major phases controlled by quorum-sensing systems [13]: virulence that allows the bacteria to invade and kill the host [14], necrotrophism which permits the bacteria to feed on the cadaver [11], and sporulation. These processes were reported in insects using fluorescent reporters to detect the activity of the regulators responsible for these states at the cell level [15]. Sporulation was shown to only occur in a part of the subpopulation that had activated the necrotrophic regulon. This is due to the dual nature of the NprR regulator that acts as an activator of the necrotrophic regulon when bound to its cognate signaling peptide NprX, and as a phosphatase negatively regulating sporulation in its apo-form [16]. Necrotrophism was reported to be activated during the whole experiment time-span (*i.e.* 4 days) in bacteria that did not engage in sporulation. A category of cells, which did not express the necrotrophic or the sporulation reporters in the host, was identified and designated Nec$^-$/Spo [15,17]. Most of these bacteria were identified as viable using a cell death marker at 3 dpi and the results suggested that they were not in exponential or stationary phase [18], (and unpublished).

In this study, we investigated the composition of the bacterial population during the late stages of an infection as well as the characteristics and the proportion of the non-sporulated bacterial population in the *B. thuringiensis*/*G. mellonella* infection model. We used an unstable fluorescent reporter coupled to flow cytometry to determine the actual duration of necrotrophism. We also examined the metabolic state of the Spo$^-$ cells using protein synthesis and growth recovery assays on rich or insect-based medium. We performed a transcriptomic analysis of this subpopulation at 7 dpi that revealed a signature profile of this state.

MATERIALS AND METHODS

Bacterial strains and growth conditions

The acrystalliferous *Bacillus thuringiensis* 407 Cry$^-$ strain (*B. thuringiensis* 407$^-$) [19] was used as the parental strain to create all the strains used in this study. *Escherichia coli* strain DH5α

94 [20] was used as the host strain for plasmid construction. *E. coli* strain ET12567 [21] was used
95 to prepare DNA prior to electroporation in *B. thuringiensis*. Cells were grown under shaking at
96 30°C or 37°C in LB medium (1% tryptone, 0.5% yeast extract, 1% NaCl) or HCT medium
97 (0.7% casein hydrolysate, 0.5% tryptone, 0.68% KH2PO4, 0.012% MgSO4·7H2O, 0.00022%
98 MnSO4·4H2O, 0.0014% ZnSO4·7H2O, 0.008% ferric ammonium citrate, 0.018%
99 CaCl2·4H2O, pH 7.2). The bacteria were stored at -80°C in LB containing 15% glycerol.
100 When required, the medium was supplemented with antibiotics at the following concentrations:
101 100 µg/mL ampicillin (for *E. coli*), 200 µg/mL kanamycin, 10 µg/mL erythromycin (for
102 *B. thuringiensis*).
103
104 ***Plasmids and strains construction***
105 DNA manipulations are detailed in the supplemental material. All the plasmids, strains and
106 oligonucleotide primers used in this study are listed in Tables S1, S2 and S3 in the supplemental
107 material.
108
109 ***Infection of* Galleria mellonella**
110 Intrahemocoelic injection experiments with *Galleria mellonella* were carried out as described
111 previously [14]. Briefly, last instar larvae were infected by intrahaemocœlic injections with
112 2.10^4 vegetative cells in exponential phase (OD_{600}=1). Inocula were numerated after plating
113 onto LB agar medium. Infected larvae were incubated at 30°C under a Nikon CoolPix P1 on
114 time-lapse photography mode and pictures were taken every 10 min to determine the time of
115 death for each larva. Larvae that died within the same hour were used for each time point. A
116 larva was considered dead at the time its movements stopped if followed by melanization (see
117 supplemental material for details, fig S1.).
118 ***Extraction of* B. thuringiensis *from* G. mellonella *cadavers***

119 Isolation of bacteria from insect cadavers was adapted from Verplaetse et al., 2015, [15].
120 Cadavers were crushed with a 1 mL tip in a 1.5 mL Eppendorf tube. 1 mL of saline was added
121 and the tube was vortexed. 750 µL of the suspension were transferred to a new 1.5 mL tube and
122 centrifuged for 45 sec at 13000 rpm. The pellet was resuspended in 750 µL of saline and loaded
123 in a 1 mL syringe fitted with a cotton filter in order to isolate bacterial cells from cadaver debris.
124 The filtrate was then centrifuged for 30 sec at 13000 rpm, fixed in 4% formaldehyde in saline
125 for 15 min, washed in saline, resuspended in GTE buffer [22] and kept at 4°C until flow
126 cytometric or microscopy analysis.
127
128 ***Flow cytometric analysis***
129 Bacteria were diluted in filtered saline and fluorescent events were measured on a CyFlow
130 Space cytometer (Sysmex Partec, France). Specifications of the apparatus and flow cytometric
131 analyses are described in the supplemental material.
132
133 ***Microscopy***
134 Bacteria were observed with an AxioObserver.Z1 Zeiss inverted fluorescence microscope with
135 a Zeiss AxioCam MRm digital camera and with Zeiss fluorescence filters. GFP, 5(6)-CFDA,
136 DiBAC4(3), Sytox Green were imaged using the 38 HE filter (excitation: BP 470/40, beam
137 splitter: FT 495, emission: 525/50) and mCherry was imaged using the 45 HE filter (excitation:
138 BP 590/20, beam splitter: FT 605, emission: 620/14). Images were processed using the ZEN
139 software package (Zeiss).
140
141 ***Sporulation assay***
142 The sporulated population was assessed by plating and by flow cytometry. Each larva cadaver
143 was ground in 3 mL of saline on ice using an T10 Ultra-Turaxx apparatus. The volume was then

144 adjusted to 10 mL. To determine the number of total cells and the number of heat-resistant
145 spores, the bacteria were enumerated by plating on LB agar plates following serial dilutions
146 before and after heat treatment at 80°C for 12 min. For flow cytometry, fixed bacteria (as
147 described above) harboring the red fluorescent sporulation reporter *PspoIIQ-mCherry* were
148 analyzed. Red fluorescent events were counted among the total cell count to calculate the
149 percentage of sporulation.
150
151 ***Induction of gfp expression***
152 Bacteria were extracted from insect cadavers as described above or were harvested from HCT
153 cultures at 30°C at OD_{600}=1 (exponential phase of growth) and OD_{600}=6 (stationary phase of
154 growth) *via* centrifugation at 13000 rpm for 30 sec, washed once in saline and resuspended in
155 conditioned HCT medium (obtained after filtration of a 10 h culture of *B. thuringiensis* 407^- in
156 HCT) to preserve bacteria while preventing cell growth. Half of the suspension was
157 supplemented with xylose at 25 mM final concentration. For each sample, an aliquot was fixed
158 as described above at the time of xylose addition and after 1 and 2 h of incubation with shaking
159 at 30°C. The samples were kept at 4°C until flow cytometric or microscopy analysis.
160
161 ***Growth recovery assessment of the bacteria extracted from insect cadavers***
162 Culturability was assessed by plating the bacteria on two different media, LB agar and Insect
163 agar, and by time-lapse microscopy. The bacteria were extracted from insect cadavers as
164 described above or were harvested from *in vitro* cultures in LB at 30°C at OD_{600}=1 (exponential
165 phase), OD_{600}=8 (stationary phase) and from a 48 h culture (composed of about 65% of spores)
166 *via* centrifugation at 13000 rpm for 30 sec, washed once in saline, serial diluted and plated onto
167 LB plates containing erythromycin. 16 hours after incubation at room temperature, colonies
168 were photographed with a Canon Eos 750D under a binocular stereo microscope Leica

169 MZFLIII. Colony area was determined using the Image J software [23].

170 To prepare Insect agar plates, 12 larvae cadavers were harvested at 7 dpi and crushed in 50 mL
171 saline then filtered as described above. Agar prepared in saline was then added at a final
172 concentration of 1.5%. The bacteria extracted from insect larvae or harvested from LB cultures,
173 in the same manner as above, were serial diluted and plated onto LB plates supplemented with
174 erythromycin and Insect agar plates supplemented with erythromycin. Colonies were counted
175 16 hours after incubation at room temperature for LB plates and after 4 days for Insect agar
176 plates.

177 For time lapse microscopy, medium pads were prepared with LB supplemented with 1%
178 agarose to fill a 125-µl GeneFrame (Thermo Fisher Scientific, Waltham, MA, U.S.A.). After
179 polymerization, 2-mm-wide strips were cut and three strips were placed in a new gene frame.
180 Bacteria were extracted from insect larvae or harvested from LB cultures as described above
181 and washed in saline. 2 µL of cells were then pipetted onto the strips before the frame was
182 sealed with a coverslip. *B. thuringiensis* development was monitored at 30°C in a temperature-
183 controlled chamber with the microscope described above. Phase-contrast and fluorescence
184 images were taken every hour for 5 h. Only bacteria extracted from insect cadavers at 0 h were
185 assigned to a category (elongation, division, lysis, inactivity). Newly-formed daughter cells
186 were excluded from the analysis.

187

188 ***Molecular dye staining***

189 Bacterial cells were harvested from LB cultures or insect cadavers as described above and
190 resuspended in 1 mL of saline. Samples were diluted to 10^7 cells/mL in filtered saline
191 supplemented or not with one of the dyes. 5(6)-CFDA (Biotium, Fremont, CA, USA),
192 DiBAC4(3) (Sigma-Aldrich, Saint-Louis, MO, USA) and Sytox Green (Invitrogen, Eugene,
193 OR, USA) were suspended in DMSO and used at a final concentration of 5 µM (5(6)-CFDA)

194 or 0.5 µM (DiBAC4(3) and Sytox Green). Cells were incubated at room temperature for 15
195 min in the dark. Stained samples were washed once in saline before flow cytometric or
196 microscopy analysis. Unstained and heat-shocked cells at 90°C for 15 min were used as control.
197

198 ***RNA-Seq analysis***

199 RNA was extracted from shaken liquid cultures and from dead larvae at 7 dpi as
200 described in the supplemental material. Nanodrop and Bioanalyzer instruments were used for
201 quantity and quality controls (6,8 ≤ RINs ≤ 10). Disrupting cells broke Spo^- bacteria and left
202 spores intact. Moreover, extraction of RNA from spore preparations using our protocol resulted
203 in a very low yield of poor quality. However, we can not exclude a minute contamination with
204 RNA from spores.
205 Library preparation including ribosomal RNA depletion (RiboZero) and sequencing was
206 performed by the I2BC platform (Gif-sur-Yvette, France). Sequencing was conducted on an
207 Illumina NextSeq machine using NextSeq 550/500 Mid Output Kit v2 to generate paired end
208 reads (2x75).
209 Data processing was performed by the I2BC platform including the following steps:
210 demultiplexing (with bcl2fastq2-2.18.12), adapter trimming (Cutadapt 1.15), quality control
211 (FastQC v0.11.5), mapping (BWA v0.6.2-r126) against *B. thuringiensis* 407 strain. This
212 generated between 9 M and 18 M of uniquely mapped reads per sample and counts for 6530
213 genes. Differentially expressed genes (DEG) were determined using the R package "DESeq2"
214 (v1.30.1) to estimate p-values and log2 fold-changes. DEG with padj ≤ 10^{-2} and log2FC≤-2 or
215 log2FC ≥ 2 were used for further analyses. Gene expression data are being deposited at the
216 public repository Gene Expression Omnibus.
217 Using the functional re-annotation database available in the laboratory (see details in
218 supplemental materials) of the *B. thuringiensis* 407 genome (chromosome: INSDC

CP003889.1, plasmids: INSDC CP003890.1 to CP003898.1), GO terms, COG letters and *B. subtilis* homologous genes were assigned to our data-set with Microsoft SQL server 2019. Venn Diagrams were constructed with Venny 2.1.0 [24], 2007-2015 https://bioinfogp.cnb.csic.es/tools/venny/index.html). Using Subtiwiki [25], KEGG orthology database [26] and COG letters, we retrieved genes from these functional categories: oxidative stress, iron homeostasis, DNA recombination and repair, necrotrophism, sporulation, and germination (see supplemental material, table S4, S5, S6, for necrotrophism, sporulation and germination, respectively). Histograms and heatmaps of DEG according to these functional categories were then constructed using Prism 8 software (GraphPad).

Statistical analysis

The data were analyzed using the Prism 8 software (GraphPad).

231 **RESULTS**

232 ***Non-sporulated bacteria survive in insect cadavers for at least 14 days post-infection***

233 A previous study recorded the sporulation rate of *B. thuringiensis* in insect larvae cadavers and
234 showed that heat-resistant spores were detected 24 hpi and reached a plateau at 30% of the
235 bacterial population from 48 hpi until the end of the experiment 4 dpi [11]. This result indicated
236 that a large part of the bacterial population was able to survive for 4 days in these conditions
237 without resorting to sporulation. In order to determine if the non-sporulating cells persisted
238 during a longer period of time, and if the sporulation rate remained constant, we monitored the
239 fate of the bacterial population during 14 days using two complementary methods. *B.*
240 *thuringiensis* cells harboring P*spoIIQ'mcherry*, a transcriptional fusion between the promoter
241 of *spoIIQ*, a sporulation gene activated when the cells are committed to sporulation [27], and
242 the *B. thuringiensis*-optimized *mcherry* fluorescent reporter gene [15], were injected into
243 *G. mellonella* larvae. Sporulation was then assayed by plating and by flow cytometry (as
244 described in the Materials and Methods section). In our conditions, flow cytometry analysis of
245 P*spoIIQ'mCherry* cannot discriminate between bacteria irreversibly engaged in sporulation and
246 sporulated cells as the mCherry protein remains fluorescent in spores. In the plating assay, we
247 cannot exclude that some spores will not be able to germinate and form colonies on LB agar
248 plates. These two methods were therefore implemented to give the closest assessement of the
249 sporulated and non-sporulated subpopulations. Larvae died between 8 to 12 hpi (fig S1) and
250 bacteria were extracted from insect cadavers from 16 hpi to 14 dpi for analysis. The plating
251 assay showed that the total number of CFU per larva remained stable during 14 dpi (fig S2).
252 mCherry-positive bacteria (Fig 1.a and 2.a) and heat-resistant spores (Fig. S2) were detected
253 starting 1 dpi and represented about 40 and 50 % of the total population, respectively.
254 Accordingly, microscopy results indicate that the mCherry-positive events mainly correspond
255 to spores from the third day post-infection onwards (fig S2 and data not shown). The sporulation

256 rate remained stable during 14 days and was comprised between 30% and 55% indicating that
257 up to 70% of the cells could be in a non-sporulated form. We cannot exclude that germination
258 occurred in insect cadavers as a few spores had lost their refringence and remained fluorescent
259 when observed by microscopy (data not shown). However less than 5% of the bacteria
260 presented this profile (data not shown). Comparison of the data using a Bland-Altman plot (fig
261 2.b) showed that the results obtained using both methods are similar. Indeed, the bias value is
262 3.2 and the SD of bias 7.3, indicating that there is less than 10% difference in the sporulation
263 percentage when comparing plating and flow cytometry. This indicates that both methods are
264 equivalent for evaluating sporulation in these conditions. Taken together, these results show that
265 sporulation is not the only survival strategy in insect cadavers even in late-infection stages.
266
267 ***Necrotrophism is a transient state occurring at early stages of survival in insect cadavers***
268 To assess the proportion of bacteria in the necrotrophic state during the late stages of infection
269 in insect larvae, we monitored this state for 14 dpi using a transcriptional fusion between the
270 promoter of *nprA*, an NprR-regulated gene [28], and the reporter gene $gfp_{Bte}AAV$, encoding an
271 unstable Gfp [18]. This reporter gene was previously used to detect vegetative cells *in vivo* and
272 showed its relevance as a molecular tool to assess transient gene expression during infection
273 [18]. We associated this construct to the P*spoIIQ'mcherry* fusion. This combination of reporters
274 allowed us to determine the fraction of the population that was able to persist in the late stages
275 of infection without entering sporulation or activating the necrotrophism pathway.
276 *G. mellonella* larvae were infected by intrahemocoelic injection with the Bt (pP*nprA'*$gfp_{Bte}AAV$-
277 P*spoIIQ'mCherry*) strain. Figure 2 shows that expression of the P*nprA'*$gfp_{Bte}AAV$ fusion started
278 between 16 and 18 hpi with about 30% of the bacteria in the necrotrophic state (Nec^+) at 18 hpi.
279 The number of Nec^+ bacteria peaked at 20 hpi to near 60% and decreased to around 30% at 24
280 hpi. Expression of the P*spoIIQ'mCherry* fusion started between 22 and 24 hpi with about 20%

281 of the bacteria expressing the sporulation reporter only (Spo^+) and 15% of the population
282 expressing both the necrotrophic and sporulation reporter (Nec^+/Spo^+). At 2 dpi the total number
283 of Nec^+ and Nec^+/Spo^+ bacteria decreased to about 10% of the population and remained at that
284 level until the end of the experiment. These data show that necrotrophism is a transient state in
285 which the bacteria remain during a limited period after the death of their host. Furthermore, our
286 results reveal that the previously reported proportion of Nec^-/Spo^- cells was underestimated.
287
288 ***The majority of the non-sporulated late-infection stage bacteria present cellular vitality***
289 We analyzed the behavior and features of the Spo^- bacteria during infection using molecular
290 dyes to assess bacterial vitality. We used three commercial dyes to examine different vitality
291 features of these bacteria: enzymatic activity by assessing esterase activity with 5(6)-CFDA (fig
292 3.a), membrane potential with DiBAC4(3) (fig 3.b) and membrane integrity with Sytox Green
293 (fig 3.c) [29]. Sytox Green staining was previouslysuccessfully used on cells extracted from
294 insect cadavers to detect mortality among the 3 dpi non-necrotrophic cells [18]. Strain Bt
295 (pP*spoIIQ'mCherry*) cultured in LB and harvested in exponential growth phase (Expo) and
296 stationary growth phase (Stat), or extracted from insect cadavers at 1, 3 and 7 dpi, was incubated
297 with the molecular dyes listed above. Cells were then analyzed by flow cytometry (fig 3) and
298 microscopy (fig S4) to quantify the stained Spo^- cells. The results show that 5(6)-CFDA stained
299 90% of Expo and Stat cells, and 67% to 72% of insect cadavers cells (fig 3). However, this
300 difference was not statistically significant. Less than 16% of Expo and Stat cells and
301 approximately 30% of insect cadavers cells were marked with DiBAC4(3) and Sytox Green
302 (fig 3.b and 3.c). Bacteria extracted from insect cadavers presented a more heterogeneous
303 profile as the percentage of marked cells ranged from 15% to 60% of the Spo^- bacteria. Our
304 results indicate that a portion of the Spo^- cells extracted from insect cadavers was damaged, but
305 the majority of these bacteria presented esterase activity, membrane polarization and membrane

306 integrity, indicating cellular vitality.

307

308 ***Protein production induction is delayed in non-sporulated late-infection stage bacteria***

309 To further assess the physiological state of the 7 dpi bacteria, we examined the metabolic
310 activity of these cells by recording their protein synthesis ability. We designed a strain harboring
311 the transcriptional fusion P*x'gfp*$_{Bte}$ between a xylose-inducible promoter and a Gfp-encoding
312 reporter gene associated to the sporulation reporter P*spoIIQ'mCherry*. We assessed the ability
313 of the Spo$^-$ cells to synthesize proteins by incubating them in conditioned HCT medium (HCTc)
314 supplemented with xylose for 1 and 2 h and measuring the proportion of GFP-positive and
315 mCherry-negative bacteria using flow cytometry (fig 4) coupled to microscopy observations
316 (fig S5). Expo cells and Stat cells harvested from HCT cultures at 30°C, as well as bacteria
317 extracted from insect cadavers at different time points (1, 3 and 7 dpi) were subjected to this
318 treatement. The results show that at the start of induction, almost no bacteria expressed the
319 P*x'gfp*$_{Bte}$ fusion in any of the samples, except for about 6% of the Stat and 1 dpi cells (fig 4).
320 However, approximately 70% of the Spo$^-$ Expo, Stat, 1 and 3 dpi cells, synthesized Gfp at 1 h
321 post-induction. At 2 h post-induction the proportion of bacteria expressing *gfp*$_{Bte}$ in these
322 samples slightly increased to 80%. Interestingly, the 7 dpi bacteria presented a different
323 induction profile. At 1 h post-induction, less than 15% of the Spo$^-$ bacteria were fluorescent,
324 whereas at 2 h post-induction 15% to 75% of these cells were able to produce Gfp. This result
325 indicates that the 7 dpi bacteria retain their ability to synthesize proteins, albeit with a greater
326 time delay and variability between samples than for the other bacterial conditions assayed. This
327 indicates that non-sporulating bacteria undergo physiological changes during the late infection
328 stages suggestive of a metabolic slow-down.

329

330 ***Growth recovery of late-infection stage bacteria is impaired on rich medium, in contrast to***

331 ***insect medium***

332 We performed a colony-size assay to determine whether bacteria extracted at late time points
333 from insect cadavers were able to replicate when exposed to fresh growth medium. Expo cells,
334 Stat cells, spores harvested from 48 h-LB cultures at 30°C and bacteria extracted from insect
335 cadavers at 1, 3 and 7 dpi were plated onto LB agar. Plates were photographed after 16 hours
336 of incubation at room temperature (fig 5.a) and colony size was determined as described in the
337 Materials and Methods section. The results show that colonies resulting from 3 and 7 dpi
338 bacteria, as well as *in vitro*-prepared spores, were smaller than those resulting from Expo, Stat
339 and 1 dpi cells (fig 5.a). This indicates that late-infection stage bacteria recover slower than
340 bacteria sampled at an earlier infection stage or than *in vitro*-grown bacteria. This recovery is
341 similar to that of *in vitro*-generated spores. The results might reflect a delay of growth due to
342 the germination of the spores present at 3 dpi or after. However, all the colonies were smaller
343 and therefore include the Spo^- cells, unless they are unable to form a colony. After longer
344 incubation times, all the samples displayed similar colony-size (data not shown). In order to
345 determine more precisely the behavior of the bacterial subpopulations, we also examined the
346 growth of 7 dpi bacteria at the single cell level using time-lapse microscopy. Expo, Stat and 7
347 dpi bacteria were inoculated on LB agarose strips at 30°C and the behavior of Spo^- cells was
348 followed during 5 hours (fig 5.c and 5.d). About 8 to 16% of the inoculated bacteria lysed
349 regardless of the sample. Approximately 80% of Expo and Stat cells were able to divide whereas
350 the majority of 7 dpi cells were inactive (fig 5.b). We observed elongation and growth for less
351 than 20% of the 7 dpi bacteria (fig 5.c). These results show that 7 dpi bacteria rarely divided
352 over a 5 h-time-lapse experiment which is in agreement with the slower growth recovery
353 phenotype observed on LB plates.

354 In order to determine if the late-infection stage bacteria were better adapted to a medium closer
355 to the insect cadaver environement, we performed a recovery assay on an Insect agar medium

356 prepared as described in the Materials and Methods section. Expo cells, Stat cells, spores
357 harvested from 48 h-LB cultures at 30°C and bacteria extracted from insect cadavers at 1, 3 and
358 7 dpi were plated onto Insect agar plates. Figure 5.d shows that there is a drastic drop in the
359 numbers of CFU/mL resulting from the plating of Expo and Stat cells, as well as spores, on
360 Insect agar compared to LB. Less than 0.3% of these bacteria survived on this medium. About
361 6% of the 1 dpi population was able to grow on this medium compared to LB. In sharp contrast,
362 the number of CFU/mL for 3 and 7 dpi cells was similar on both media. Taken together, these
363 results suggest that the insect cadaver is a hostile environment for bacteria and that adaptation
364 is required to survive in these conditions.
365
366 ***Transcriptomic profile of late-infection B. thuringiensis***
367 To determine the expression profile of the Spo^-/Nec^- cells and begin to understand how these
368 bacteria persist in the cadavers, we performed a global *in vivo* transcriptional analysis at a late
369 stage of infection using an RNA-Sequencing approach. We chose to extract RNA from the total
370 population at the 7 dpi time-point that presented very few Nec^+ bacteria (fig 2) and we verified
371 that RNA was only poorly extracted from spores, thus preventing a biais in our analysis (see
372 Materials and Methods section). We compared the transcriptome of 7 dpi bacteria to Expo and
373 Stat bacteria grown in LB medium. The transcriptome of the Stat and Expo bacteria grown in
374 LB medium was also compared to identify genes differentially expressed in the insect
375 specifically. As presented in fig 6.a, the principal component analysis shows that the 7 dpi
376 bacteria differed substantially from both Expo and Stat cells, indicating that these cells are in a
377 different state. The results show that 484 and 203 genes were specifically up-regulated and
378 down-regulated, respectively, in the 7 dpi cells when compared to both Expo and Stat bacteria
379 (fig 6.b). We found that most of the genes belonging to the NprR regulon were down-regulated
380 when compared to Stat cells but up-regulated when compared to Expo cells (Table S4). This is

381 in accordance with the fact that a small proportion of bacteria are Nec$^+$ at 7 dpi (fig 1) while
382 necrotrophism is repressed in exponential phase and activated during stationary phase *in vitro*
383 [28]. The data also show that most sporulation and germination genes were not differentially
384 expressed, indicating that these two processes were not triggered in the subpopulation of interest
385 (Table S5, S6).
386 Most of the up-regulated genes in the 7 dpi cells are involved in inorganic ion transport and
387 metabolism, transcription, replication, recombination and repair, whereas the down-regulated
388 genes are mostly involved in cell motility, signal transduction mechanisms and cell
389 wall/membrane/envelope biogenesis (fig 6.c), the latter indicating a decrease in the growth
390 process. More than 300 differentially expressed genes were assigned to an unkown function.
391 Differentially expressed genes with the highest or lowest log2FC values were found in the
392 oxidative stress, iron homeostasis, DNA replication, recombination and repair and cell motility
393 categories (fig 6.d). Interestingly, all motility genes were down, all iron homeostasis genes were
394 up, and all oxidative stress genes were up (except for one), indicating that these mechanisms
395 are key for late infection stage survival.
396
397 ***Oxidative stress genes are specifically expressed during late-infection, in contrast to iron***
398 ***homeostasis genes expressed at all times***
399 To examine the expression profile of selected genes identified in the RNA-Seq analysis and
400 determine which of these were specific to late infection stage survival, we constructed strains
401 harboring a transcriptional fusion between the promoter region of the gene of interest and the
402 *gfp$_{Bte}$AAV* reporter gene, associated to the sporulation reporter P*spoIIQ-mCherry*. We chose
403 genes with the highest log2FC values obtained by the differential gene expression analysis in
404 the iron homeostasis and oxidative stress resistance categories. We followed the expression
405 profile of representative genes from these categories such as *ykun2* (a flavodoxin that replaces

406 ferredoxin under conditions of iron limitation), *isdE1* (involved in heme scavenging), *dhbA* (the
407 first gene of the *dhb* operon that specifies the biosynthesis of the siderophore bacillibactin
408 involved in the chelation of ferric iron from the surrounding environment), *BTB_c10430*
409 (annotated as *sigX* by KEGG orthology), *katE1* (a catalase and general stress protein) and *sodA1*
410 (a superoxide dismutase and general stress protein) [26]. P*ykun2'gfp*$_{Bte}$*AAV* and
411 P*isdE1'gfp*$_{Bte}$*AAV* were expressed from the start of the infection, and the percentage of
412 fluorescent cells among the Spo$^-$ cells was around 30% (fig 7.a and 7.b). Similarly,
413 P*dhbA'gfp*$_{Bte}$*AAV* was expressed in approximately 40% of the cells among the Spo$^-$ bacteria in
414 the 1, 3 and 7 dpi samples (fig 7.c). For the reporter P*BTB_c10430'gfp*$_{Bte}$*AAV* less than 20% of
415 the 1 and 3 dpi Spo$^-$ cells were Gfp-positive. At 7 dpi, around 40% of the Spo$^-$ cells produced
416 Gfp, indicating a specific activation of *BTB_c10430* during in late infection survival (fig 7.d).
417 P*katE1'gfp*$_{Bte}$*AAV* and P*sodA1'gfp*$_{Bte}$*AAV* were specifically expressed in 7 dpi cells with about
418 65% of green fluorescent Spo$^-$ cells for the former and 80% for the latter (fig 7.c). As expected,
419 none of these reporters were expressed in Expo and Stat cells. Altogether, these results indicate
420 that iron homeostasis is important from the start of the infection whereas an oxidative stress
421 response is mounted as the bacteria spend more time in the cadaver environment.
422

423 **DISCUSSION**

424 Our study reports the characterization of a physiological state that procures the sporulating
425 entomopathogenic Gram-positive bacterium *B. thuringiensis* specific properties allowing its
426 persistence in the host environment in a non-sporulated form. We analyzed the phenotypic
427 properties and transcription profile of the Spo$^-$ *B. thuringiensis* cells in the context of an
428 infection in *G. mellonella* larvae. These larvae are natural hosts for the *B. thuringiensis* species,
429 but they are also widely used as an alternative to mammalian models of infection to study
430 bacterial virulence and host colonization [30,31].

431 The RNA-Seq analysis showed that the motility genes were down-regulated in 7 dpi bacteria
432 compared to *in-vitro*-grown cells, and that the motility repressor-encoding gene *mogR* [32] was
433 up-regulated in 7 dpi bacteria compared to exponentially growing cells. Similarly, the biofilm-
434 associated genes *calY*, *tasA* and the *eps2* locus [33,34], were up-regulated compared to
435 exponentially growing cells. These data suggest that the late-infection stage bacteria form a
436 biofilm which might confer them an advantage for long-term survival considering the resistance
437 properties of these structures [35]. The most represented categories among the up-regulated
438 transcripts in 7 dpi bacteria compared to *in vitro*-grown cells are the oxidative stress response,
439 DNA recombination, replication and repair in addition to iron homeostasis. The expression of
440 uptake systems for iron, as well as biosynthesis and uptake of the endogenous siderophore
441 bacillibactin was shown to be activated by iron limitation in *B. cereus* [36]. During an infection,
442 the host is considered to be an iron-depleted environment and bacteria need to deploy strategies
443 to scavenge this element, such as the activation of the Fur regulon [37,38]. This is consistent
444 with the activation of the iron homeostasis genes *dhbA* and *isdE1*, belonging to this regulon,
445 during all stages of the infection. Iron is essential for the function of various proteins and iron
446 homeostasis was previously reported as being important for *B. cereus* pathogenesis in the first
447 stages of *G. mellonella* infection by oral gavage [39]. However, this metal is also a potential
448 hazard in combination with compounds such as H_2O_2 because the reaction between the two
449 products generates reactive oxygen species (ROS) that can be harmful by damaging cellular
450 components such as DNA or proteins with [Fe-S] clusters [40]. Several studies have linked iron
451 homeostasis and DNA repair to a response to oxidative stress and showed the upregulation of
452 these gene categories upon H_2O_2 exposure [41,42], and it was recently reported that H_2O_2 was
453 produced in the hemolymph of *G. mellonella* during *Salmonella enterica* infection [43].
454 Moreover, the melanization defense reaction that occurs after the insect infection liberates ROS
455 and might last for several days [44–46]. Aerobic metabolism also generates endogenous

456 oxidative stress if O_2 is not completely reduced during respiration and a secondary oxydative
457 stress response can also be triggered when *Bacillus* encounter unfavorable conditions in an
458 aerobic environment [47]. All these stresses are counteracted by the action of proteins such as
459 catalases (Kat), superoxide dismutases (SodA) or DNA-binding ferroxidases (Dps) [48,49], all
460 of which are overexpressed in 7 dpi bacteria. RNA-Seq analysis also revealed that the
461 BTB_c10430 locus, annotated as encoding the SigX protein [26], is specifically up-regulated
462 in 7 dpi bacteria. SigX belongs to the extracytoplasmic function (ECF) sigma factor family that
463 helps maintain cell envelope homeostasis and activate resistance to agents that can compromise
464 the integrity of the envelope, the first defense against environmental threats [50]. A *B. subtilis*
465 *sigX* deletion mutant was shown to be sensitive to oxidative stress [51] . Further investigations
466 should examine the involvement of this regulatory protein in the maintenance of
467 *B. thuringiensis* in insect cadavers. It would also be informative to determine if the oxidative
468 stress response triggered in the late-infection stage bacteria is due to the cadaver environment,
469 to an excessive iron uptake or to a combination of the two and to understand the role of the
470 oxidative stress response in the resistance of *B. thuringiensis* during long-term infection.
471 *B. thuringiensis* is able to overcome the immune defenses of *G. mellonella*, to multiply and to
472 completely invade its host in less than 24 hpi [11,52,53], (this study and unpublished). It was
473 shown that the bacteria engage in necrotrophism after the death of the larva by activating the
474 NprR regulon that includes genes encoding chitinases, proteases and oligopeptide permeases
475 [11,15]. Activation of this regulon seemed to last throughout the duration of the infection [15]
476 and an *nprR* deletion mutant was unable to survive in the cadaver suggesting that the regulon
477 was required for long-term survival. However, we showed here that necrotrophism is a transient
478 state limited to the first stages of survival in the cadaver. We propose that this state allows *B.*
479 *thuringiensis* to scavenge the nutrients present in the cadaver shortly after the insect death, then
480 the bacteria enter different pathways, potentially triggered by a stress signal such as nutrient

depletion, that allow for their persistence in the host. A subpopulation enters the differentiation pathway leading to sporulation, while another engages in a metabolic slow-down that accentuates with the increase of exposure time to the cadaver environment. This subpopulation also showed resistance to the cadaver environment which proved hostile for *in vitro*-grown bacteria as well as *in-vitro* generated spores.

Altogether, these results show that non-sporulated late-infection stage *B. thuringiensis* are resilient cells able to resist in a harsh environment and suggest that this adaptation relies mainly on the activation of stress resistance genes as well as entering a metabolic slow-down. The fitness advantages conferred by the phenotypic heterogeneity of the *B. thuringiensis* population during infection and, in particular, by the co-existence of spores and of the non-sporulated form able to survive for a prolonged period in a host cadaver, still need to be elucidated. Studying the mechanisms that govern this state will provide valuable fundamental knowledge about the lifecycle of these bacteria and might lead to the development of new strategies to combat sporulating pathogenic species.

CONFLICT OF INTEREST STATEMENT

The authors declare that the research was conducted in the absence of any commercial or financial relationships that could be construed as a potential conflict of interest.

ACKNOWLEDGEMENTS

The authors are indebted to Christophe Buisson for insect rearing. This work has benefited from the facilities and expertise of the high throughput sequencing core facility of I2BC (Centre de Recherche de Gif – http://www.i2bc.paris-saclay.fr/) and the authors thank Delphine Naquin for primary analysis. We are grateful to Tarek Toukabri, Agnès Réjasse and Sébastien Gélis-Jeanvoine and Yan Jaszczyszyn for their help with the RNA-Seq experiment and analysis. The

CyFlow Space flow cytometer was funded by the DIM Astrea (French regional program Ast11 0137). HT was the recipient of a doctoral grant from the ministry of French higher education, delivered by the Doctoral School ABIES at AgroParisTech–Université Paris Saclay. This work was supported by the MICA department of INRAE (French National Research Institute for Agriculture, Food and Environment).

REFERENCES

[1] Galperin MY. Genome Diversity of Spore-Forming Firmicutes. Microbiol Spectr 2013;1. https://doi.org/10.1128/microbiolspectrum.TBS-0015-2012.

[2] Hilbert DW, Piggot PJ. Compartmentalization of Gene Expression during *Bacillus subtilis* Spore Formation. Microbiol Mol Biol Rev 2004;68:234–62. https://doi.org/10.1128/MMBR.68.2.234-262.2004.

[3] Setlow P. Spore Resistance Properties. Microbiol Spectr 2014;2:2.5.11. https://doi.org/10.1128/microbiolspec.TBS-0003-2012.

[4] Horneck G, Bücker H, Reitz G. Long-term survival of bacterial spores in space. Advances in Space Research 1994;14:41–5. https://doi.org/10.1016/0273-1177(94)90448-0.

[5] Stragier P, Losick R. Cascades of sigma factors revisited. Mol Microbiol 1990;4:1801–6. https://doi.org/10.1111/j.1365-2958.1990.tb02028.x.

[6] Gray DA, Dugar G, Gamba P, Strahl H, Jonker MJ, Hamoen LW. Extreme slow growth as alternative strategy to survive deep starvation in bacteria. Nat Commun 2019;10:890. https://doi.org/10.1038/s41467-019-08719-8.

[7] Piggot PJ, Coote JG. Genetic aspects of bacterial endospore formation. Bacteriol Rev 1976;40:908–62. https://doi.org/10.1128/br.40.4.908-962.1976.

[8] Molle V, Fujita M, Jensen ST, Eichenberger P, González-Pastor JE, Liu JS, et al. The Spo0A regulon of Bacillus subtilis: The Spo0A regulon. Molecular Microbiology

2003;50:1683–701. https://doi.org/10.1046/j.1365-2958.2003.03818.x.

[9] Rousset L, Alpha-Bazin B, Château A, Armengaud J, Clavel T, Berge O, et al. Groundwater promotes emergence of asporogenic mutants of emetic *Bacillus cereus*. Environ Microbiol 2020;22:5248–64. https://doi.org/10.1111/1462-2920.15203.

[10] Antequera-Gómez ML, Díaz-Martínez L, Guadix JA, Sánchez-Tévar AM, Sopeña-Torres S, Hierrezuelo J, et al. Sporulation is dispensable for the vegetable-associated life cycle of the human pathogen *Bacillus cereus*. Microb Biotechnol 2021;14:1550–65. https://doi.org/10.1111/1751-7915.13816.

[11] Dubois T, Faegri K, Gélis-Jeanvoine S, Perchat S, Lemy C, Buisson C, et al. Correction: Necrotrophism Is a Quorum-Sensing-Regulated Lifestyle in Bacillus thuringiensis. PLoS Pathog 2016;12:e1006049. https://doi.org/10.1371/journal.ppat.1006049.

[12] Ehling-Schulz M, Lereclus D, Koehler TM. The Bacillus cereus Group: Bacillus Species with Pathogenic Potential. Microbiol Spectr 2019;7. https://doi.org/10.1128/microbiolspec.GPP3-0032-2018.

[13] Slamti L, Perchat S, Huillet E, Lereclus D. Quorum Sensing in Bacillus thuringiensis Is Required for Completion of a Full Infectious Cycle in the Insect. Toxins 2014;6:2239–55. https://doi.org/10.3390/toxins6082239.

[14] Salamitou S, Ramisse F, Brehélin M, Bourguet D, Gilois N, Gominet M, et al. The plcR regulon is involved in the opportunistic properties of Bacillus thuringiensis and Bacillus cereus in mice and insects. Microbiology 2000;146:2825–32. https://doi.org/10.1099/00221287-146-11-2825.

[15] Verplaetse E, Slamti L, Gohar M, Lereclus D. Cell Differentiation in a Bacillus thuringiensis Population during Planktonic Growth, Biofilm Formation, and Host Infection. MBio 2015;6:e00138-15. https://doi.org/10.1128/mBio.00138-15.

[16] Perchat S, Talagas A, Poncet S, Lazar N, Li de la Sierra-Gallay I, Gohar M, et al. How

Quorum Sensing Connects Sporulation to Necrotrophism in Bacillus thuringiensis. PLoS Pathog 2016;12:e1005779. https://doi.org/10.1371/journal.ppat.1005779.

[17] Verplaetse E, Slamti L, Gohar M, Lereclus D. Two distinct pathways lead Bacillus thuringiensis to commit to sporulation in biofilm. Res Microbiol 2017;168:388–93. https://doi.org/10.1016/j.resmic.2016.03.006.

[18] Ben Rejeb S, Lereclus D, Slamti L. Analysis of abrB Expression during the Infectious Cycle of Bacillus thuringiensis Reveals Population Heterogeneity. Front Microbiol 2017;8:2471. https://doi.org/10.3389/fmicb.2017.02471.

[19] Lereclus D. Transformation and expression of a cloned δ-endotoxin gene in bacillus thuringiensis. FEMS Microbiology Letters 1989;60:211–7. https://doi.org/10.1016/0378-1097(89)90511-9.

[20] Taylor RG, Walker DC, Mclnnes RR. *E.coli* host strains significantly affect the quality of small scale plasmid DNA preparations used for sequencing. Nucl Acids Res 1993;21:1677–8. https://doi.org/10.1093/nar/21.7.1677.

[21] MacNeil DJ, Gewain KM, Ruby CL, Dezeny G, Gibbons PH, MacNeil T. Analysis of Streptomyces avermitilis genes required for avermectin biosynthesis utilizing a novel integration vector. Gene 1992;111:61–8. https://doi.org/10.1016/0378-1119(92)90603-M.

[22] Vlamakis H, Aguilar C, Losick R, Kolter R. Control of cell fate by the formation of an architecturally complex bacterial community. Genes Dev 2008;22:945–53. https://doi.org/10.1101/gad.1645008.

[23] Schneider CA, Rasband WS, Eliceiri KW. NIH Image to ImageJ: 25 years of image analysis. Nat Methods 2012;9:671–5. https://doi.org/10.1038/nmeth.2089.

[24] Oliveros JC. An interactive tool for comparing lists with Venn's diagrams. Venny 21 2007. https://bioinfogp.cnb.csic.es/tools/venny/index.html (accessed April 16, 2022).

[25] Pedreira T, Elfmann C, Stülke J. The current state of SubtiWiki, the database for the model

organism Bacillus subtilis. Nucleic Acids Res 2022;50:D875–82. https://doi.org/10.1093/nar/gkab943.

[26] Kanehisa M, Sato Y, Kawashima M, Furumichi M, Tanabe M. KEGG as a reference resource for gene and protein annotation. Nucleic Acids Res 2016;44:D457-462. https://doi.org/10.1093/nar/gkv1070.

[27] Londoño-Vallejo JA, Fréhel C, Stragier P. SpoIIQ, a forespore-expressed gene required for engulfment in Bacillus subtilis. Mol Microbiol 1997;24:29–39. https://doi.org/10.1046/j.1365-2958.1997.3181680.x.

[28] Perchat S, Dubois T, Zouhir S, Gominet M, Poncet S, Lemy C, et al. A cell-cell communication system regulates protease production during sporulation in bacteria of the Bacillus cereus group. Mol Microbiol 2011;82:619–33. https://doi.org/10.1111/j.1365-2958.2011.07839.x.

[29] Kumar SS, Ghosh AR. Assessment of bacterial viability: a comprehensive review on recent advances and challenges. Microbiology (Reading) 2019;165:593–610. https://doi.org/10.1099/mic.0.000786.

[30] Tsai CJ-Y, Loh JMS, Proft T. Galleria mellonella infection models for the study of bacterial diseases and for antimicrobial drug testing. Virulence 2016;7:214–29. https://doi.org/10.1080/21505594.2015.1135289.

[31] Fedhila S, Buisson C, Dussurget O, Serror P, Glomski IJ, Liehl P, et al. Comparative analysis of the virulence of invertebrate and mammalian pathogenic bacteria in the oral insect infection model Galleria mellonella. J Invertebr Pathol 2010;103:24–9. https://doi.org/10.1016/j.jip.2009.09.005.

[32] Smith V, Josefsen M, Lindbäck T, Hegna IK, Finke S, Tourasse NJ, et al. MogR Is a Ubiquitous Transcriptional Repressor Affecting Motility, Biofilm Formation and Virulence in Bacillus thuringiensis. Front Microbiol 2020;11:610650.

https://doi.org/10.3389/fmicb.2020.610650.

[33] Candela T, Fagerlund A, Buisson C, Gilois N, Kolstø A-B, Økstad OA, et al. CalY is a major virulence factor and a biofilm matrix protein. Mol Microbiol 2019;111:1416–29. https://doi.org/10.1111/mmi.14184.

[34] Caro-Astorga J, Frenzel E, Perkins JR, Álvarez-Mena A, de Vicente A, Ranea JAG, et al. Biofilm formation displays intrinsic offensive and defensive features of Bacillus cereus. NPJ Biofilms Microbiomes 2020;6:3. https://doi.org/10.1038/s41522-019-0112-7.

[35] Lin Y, Briandet R, Kovács ÁT. Bacillus cereus sensu lato biofilm formation and its ecological importance. Biofilm 2022;4:100070. https://doi.org/10.1016/j.bioflm.2022.100070.

[36] Hayrapetyan H, Siezen R, Abee T, Nierop Groot M. Comparative Genomics of Iron-Transporting Systems in Bacillus cereus Strains and Impact of Iron Sources on Growth and Biofilm Formation. Front Microbiol 2016;7:842. https://doi.org/10.3389/fmicb.2016.00842.

[37] Fedhila S, Daou N, Lereclus D, Nielsen-LeRoux C. Identification of *Bacillus cereus* internalin and other candidate virulence genes specifically induced during oral infection in insects: *Bacillus cereus* internalin. Molecular Microbiology 2006;62:339–55. https://doi.org/10.1111/j.1365-2958.2006.05362.x.

[38] Daou N, Buisson C, Gohar M, Vidic J, Bierne H, Kallassy M, et al. IlsA, a unique surface protein of Bacillus cereus required for iron acquisition from heme, hemoglobin and ferritin. PLoS Pathog 2009;5:e1000675. https://doi.org/10.1371/journal.ppat.1000675.

[39] Consentino L, Rejasse A, Crapart N, Bevilacqua C, Nielsen-LeRoux C. Laser capture microdissection to study Bacillus cereus iron homeostasis gene expression during Galleria mellonella in vivo gut colonization. Virulence 2021;12:2104–21. https://doi.org/10.1080/21505594.2021.1959790.

[40] Cornelis P, Wei Q, Andrews SC, Vinckx T. Iron homeostasis and management of oxidative stress response in bacteria. Metallomics 2011;3:540–9. https://doi.org/10.1039/c1mt00022e.

[41] Fu J, Qi L, Hu M, Liu Y, Yu K, Liu Q, et al. Salmonella proteomics under oxidative stress reveals coordinated regulation of antioxidant defense with iron metabolism and bacterial virulence. J Proteomics 2017;157:52–8. https://doi.org/10.1016/j.jprot.2017.02.004.

[42] Wu M, Shan W, Zhao G-P, Lyu L-D. H2O2 concentration-dependent kinetics of gene expression: linking the intensity of oxidative stress and mycobacterial physiological adaptation. Emerg Microbes Infect 2022;11:573–84. https://doi.org/10.1080/22221751.2022.2034484.

[43] Bismuth HD, Brasseur G, Ezraty B, Aussel L. Bacterial Genetic Approach to the Study of Reactive Oxygen Species Production in Galleria mellonella During Salmonella Infection. Front Cell Infect Microbiol 2021;11:640112. https://doi.org/10.3389/fcimb.2021.640112.

[44] Nakhleh J, Christophides GK, Osta MA. The serine protease homolog CLIPA14 modulates the intensity of the immune response in the mosquito Anopheles gambiae. J Biol Chem 2017;292:18217–26. https://doi.org/10.1074/jbc.M117.797787.

[45] Cerenius L, Lee BL, Söderhäll K. The proPO-system: pros and cons for its role in invertebrate immunity. Trends Immunol 2008;29:263–71. https://doi.org/10.1016/j.it.2008.02.009.

[46] Nappi A, Poirié M, Carton Y. The role of melanization and cytotoxic by-products in the cellular immune responses of Drosophila against parasitic wasps. Adv Parasitol 2009;70:99–121. https://doi.org/10.1016/S0065-308X(09)70004-1.

[47] Mols M, Abee T. Primary and secondary oxidative stress in Bacillus. Environ Microbiol 2011;13:1387–94. https://doi.org/10.1111/j.1462-2920.2011.02433.x.

[48] Zhao L, Zhou Y, Li J, Xia Y, Wang W, Luo X, et al. Transcriptional response of Bacillus

megaterium FDU301 to PEG200-mediated arid stress. BMC Microbiol 2020;20:351. https://doi.org/10.1186/s12866-020-02039-4.

[49] Shrivastava AK, Pandey S, Dietz KJ, Singh PK, Singh S, Rai R, et al. Overexpression of AhpC enhances stress tolerance and N2-fixation in Anabaena by upregulating stress responsive genes. Biochim Biophys Acta 2016;1860:2576–88. https://doi.org/10.1016/j.bbagen.2016.07.031.

[50] Helmann JD. Bacillus subtilis extracytoplasmic function (ECF) sigma factors and defense of the cell envelope. Curr Opin Microbiol 2016;30:122–32. https://doi.org/10.1016/j.mib.2016.02.002.

[51] Huang X, Decatur A, Sorokin A, Helmann JD. The Bacillus subtilis sigma(X) protein is an extracytoplasmic function sigma factor contributing to survival at high temperature. J Bacteriol 1997;179:2915–21. https://doi.org/10.1128/jb.179.9.2915-2921.1997.

[52] Kamar R, Réjasse A, Jéhanno I, Attieh Z, Courtin P, Chapot-Chartier M-P, et al. DltX of Bacillus thuringiensis Is Essential for D-Alanylation of Teichoic Acids and Resistance to Antimicrobial Response in Insects. Front Microbiol 2017;8:1437. https://doi.org/10.3389/fmicb.2017.01437.

[53] Attieh Z, Mouawad C, Rejasse A, Jehanno I, Perchat S, Hegna IK, et al. The fliK Gene Is Required for the Resistance of Bacillus thuringiensis to Antimicrobial Peptides and Virulence in Drosophila melanogaster. Front Microbiol 2020;11:611220. https://doi.org/10.3389/fmicb.2020.611220.

681 **FIGURE LEGENDS**

682 **Figure 1. Monitoring of the sporulated subpopulation during long-term infection. a.** The
683 percentage of sporulation was determined daily for 14 days after intrahemocoelic infection of
684 *G. mellonella* with Bt (pP*nprA'gfp*$_{Bte}$*AAV*-P*spoIIQ'mCherry*) by plating onto LB agar (blue)
685 or by flow cytometry (purple). 6 larvae were crushed at the time points indicated and serial
686 dilutions of the homogenate were directly plated onto LB agar for total population numeration,
687 or after heating at 80°C during 12 minutes to account for heat-resistant spores. For the flow
688 cytometry assay, the same samples were fixed and red fluorescent events were discriminated in
689 cytograms (as described in the Materials and Methods) and counted as sporulating bacteria. The
690 total population was determined by the number of total events. Each symbol represents the data
691 relative to bacteria extracted from one larva. The data are the result of two independent
692 experiments and the error bars show the standard deviation from the mean. **b.** Bland-Altman
693 comparison plot between flow cytometry and plating sporulation assessment. The difference
694 between plating and flow cytometry is plotted on the Y axis and the average of the values
695 obtained by both method is plated on the X axis. The black line represents the bias value (3,198)
696 and dotted lines indicates the 95% limits of agreement. Data were collected from 27 larvae.

697

698 **Figure 2. Necrotrophism and sporulation promoter activities in bacterial cells during**
699 **long-term infection.** Flow cytometry analysis of Bt (pP*nprA'gfp*$_{Bte}$*AAV*-P*spoIIQ'mCherry*)
700 cells during *G. mellonella* infection. Cells were extracted from 6 larvae cadavers at the time
701 points indicated during 14 days after intrahemocoelic infection. The percentage of the total cell
702 count represented by each population was discriminated in cytograms and is presented as a
703 function of time (as described in the Materials and Methods section). Each population
704 phenotype is associated with a color: Nec$^+$ in blue for cells expressing the necrotrophic marker,
705 Spo$^+$ in pink for cells expressing the sporulation marker, Nec$^+$/Spo$^+$ in purple for cells

706 expressing both markers, ND in black for cells that do not express any of the markers used.
707 Each symbol represents bacteria extracted from one larva. The data are the result of two
708 independent experiments and the error bars show the standard deviation from the mean.
709
710 **Figure 3. Assessment of the vitality status of the non-sporulated bacteria during infection.**
711 Flow cytometry analysis of Bt (pP*spoIIQ'mCherry*) cells grown in LB medium and harvested
712 in exponential (OD_{600} = 1, dark blue) or stationnary phase (OD_{600} = 8, light blue), or extracted
713 from *G. mellonella* cadavers at 1 day (pink), 3 (dark purple) and 7 days (light purple) post-
714 infection. The samples were incubated for 10 min in the dark at RT with 5 µM 5(6)-CFDA **(a)**,
715 0,5 µM DiBAC4(3) **(b)** and 0.5 µM Sytox Green **(c)** before being subjected to analysis. The
716 percentage of marked cells among non-sporulating bacteria discriminated in cytograms (as
717 described in the Materials and Methods section) is presented as a function of time. Unmarked
718 and heat-shocked bacteria were used as controls. Each symbol represents the data relative to
719 bacteria extracted from one larva. The data are the result of three independent experiments and
720 the error bars show the standard deviation from the mean. Statistically significant differences
721 are indicated by black bars with the p-value obtained after a Kruskal-Wallis Test followed by a
722 Dunn's multiple comparison test.
723
724 **Figure 4. Induction of *gfp* expression in non-sporulated bacteria during infection.** Flow
725 cytometry analysis of Bt (pP*x'gfp*$_{Bte}$-P*spoIIQ'mCherry*) cells grown in HCT medium and
726 harvested in exponential (OD_{600} = 1, dark blue) or stationnary phase (OD_{600} = 6, light blue), or
727 extracted from *G. mellonella* cadavers at 1 day (pink), 3 (dark purple) and 7 days (light purple)
728 post-infection. The bacteria were resuspended in conditioned HCT medium supplemented with
729 25 mM xylose. Aliquots were analyzed at the time of inoculation and 1 and 2 h after the start
730 of the induction. Green-fluorescent cells among the non-sporulating bacteria were

731 discriminated in cytograms as described in the Materials and Methods section. Each symbol
732 represents the data relative to bacteria extracted from one larva. The data are the result of three
733 independent experiments and the error bars show the standard deviation from the mean.
734 Statistically significant differences are indicated by black bars with the p-value obtained after
735 a Kruskal-Wallis Test followed by a Dunn's multiple comparison test.
736
737 **Figure 5. Recovery assessment of the bacteria extracted from insect cadavers. a.** Colony
738 size analysis of Bt (pP*spoIIQ'mCherry*) cells grown in LB medium and harvested in
739 exponential (OD_{600} = 1, dark blue) or stationnary phase (OD_{600} = 8, light blue), or extracted
740 from *G. mellonella* cadavers at 1 day (pink), 3 (dark purple) and 7 days (light purple) post-
741 infection, or of an *in vitro* spore preparation in LB medium (grey). The upper panels show
742 colonies photographed under a binocular stereo microscope (see details in the Materials and
743 Methods section), 16 hours post-plating on LB agar. The scale bar represents 1 mm. Colony
744 size was then measured using ImageJ as described in the Materials and Methods section. At
745 least 145 cells were measured for each condition. Each symbol on the lower graph represents
746 one colony. The data are the results of three independent experiments and the black horizontal
747 bars indicate the mean. Statistically significant differences are indicated by black bars with the
748 p-value obtained after a Kruskal-Wallis Test followed by a Dunn's multiple comparison test. **b.**
749 Time-lapse microscopy analysis performed on bacteria spotted onto LB agarose pads. One
750 picture was taken per hour, during 5 hours. Each non-sporulating cell was affected to each of
751 the listed categories and the percentage of cells for each category was calculated. The data are
752 the result of three independent experiments. At least 145 cells were counted and the error bars
753 show the standard deviation from the mean. Statistically significant differences are indicated
754 by black bars with the p-value obtained after a Kruskal-Wallis Test followed by a Dunn's
755 multiple comparison test. **c.** Time-lapse microscopy pictures with the time scale represented

above each picture. Bacteria were false colored in pink for Spo^+ cells. Arrows point to representative bacteria of the categories listed in b. The scale bar represents 10 µm. These results are representative of three independent experiments. **d.** Growth recovery on Insect agar medium. The bacteria were spotted onto Insect agar (filled bars) or LB agar plates (open bars). The bacteria were incubated at RT and CFU were numerated the next day of plating on the latter and 3 days later on the former. Each symbol represents bacteria extracted from one larva or originating from one culture. The percentage of CFU counted on LB versus Insect agar is indicated below each cell type. The data are the result of four independent experiments and the error bars show the standard deviation from the mean.

Figure 6. Transcriptomic analysis of bacterial cells extracted from insect cadavers at 7 days post-infection. a. Principal component analysis plot of the different samples: exponential growth phase cells (dark blue), stationary growth phase cells (light blue), cells extracted from insect cadavers at 7 dpi (purple). Samples were plotted against the first two principal components calculated from the gene expression values. The axes labels indicate percentage of total variance that is explained by each component. **b.** Venn diagrams indicating the number of up-regulated and down-regulated genes in cells extracted from insect cadavers at 7 dpi compared to exponential growth phase cells (purple) or stationary growth phase cells (light blue) and in stationary growth phase cells compared to exponential growth phase cells (dark blue). The genes taken into account present a log2FC≤-2 or log2FC≥2 and an adjusted p-value≤0,01. **c.** COG analysis of genes expressed in cells extracted from insect cadavers at 7 dpi compared to exponential growth phase cells and stationary growth phase cells. Blue bars indicate up-regulated genes with a log2FC≥2, purple bars indicate down-regulated genes with a log2FC≤-2. The considered genes have an adjusted p-value≤0,01. Genes with unknown functions are not represented. **d.** Heatmaps of genes expressed in cells extracted from insect

cadavers at 7 dpi compared to exponential growth phase cells (left column), stationary growth phase cells (mid column) or in bacteria harvested in stationary growth phase compared to exponential growth phase (right column). Selected categories of differentially expressed genes are shown: oxidative stress, iron homeostasis, DNA replication recombination and repair as well as cell motility. Purple indicates low expression (log2FC ≤-2) and blue indicates high expression (log2FC≥2). ns indicates an adjusted p-value>0,01.

Figure 7. Iron homeostasis and oxidative stress resistance promoter activities during infection. Flow cytometry analysis of Bt (pP*ykuN2'gfp*$_{Bte}$*AAV*-P*spoIIQ'mCherry*) (**a**), Bt (pP*isdE1'gfp*$_{Bte}$*AAV*-P*spoIIQ'mCherry*) (**b**), Bt (pP*dhbA'gfp*$_{Bte}$*AAV*-P*spoIIQ'mCherry*) (**c**), Bt (pP*BTB_c10430'gfp*$_{Bte}$*AAV*-P*spoIIQ'mCherry*) (**d**), Bt (pP*katE1'gfp*$_{Bte}$*AAV*-P*spoIIQ'mCherry*) (**e**) and Bt (pP*sodA1'gfp*$_{Bte}$*AAV*-P*spoIIQ'mCherry*) (**f**) cells grown in LB medium and harvested in exponential (OD_{600} = 1, dark blue) or stationnary phase (OD_{600} = 8, light blue), or extracted from *G. mellonella* cadavers at 1 day (pink), 3 (dark purple) and 7 days (light purple) pi. Green fluorescent cells among the non-sporulating bacteria were discriminated in cytograms as described in the Materials and Methods section. Each symbol represents the data relative to bacteria extracted from one larva. The data are the result of two independent experiments and the error bars show the standard deviation from the mean. Statistically significant differences are indicated by black bars with the p-value obtained after a Kruskal-Wallis Test followed by a Dunn's multiple comparison test.

FIGURES

Figure 1

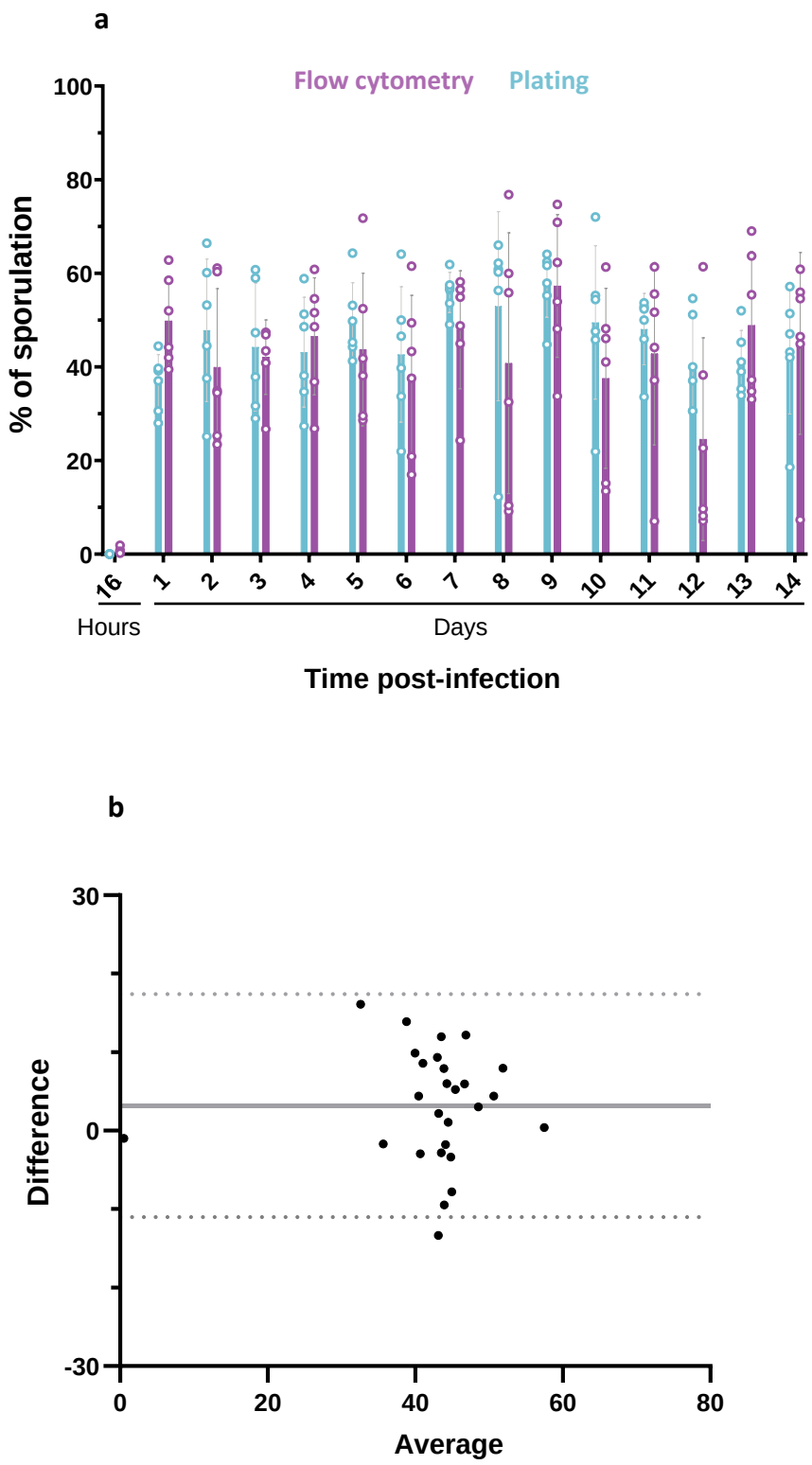

Figure 2

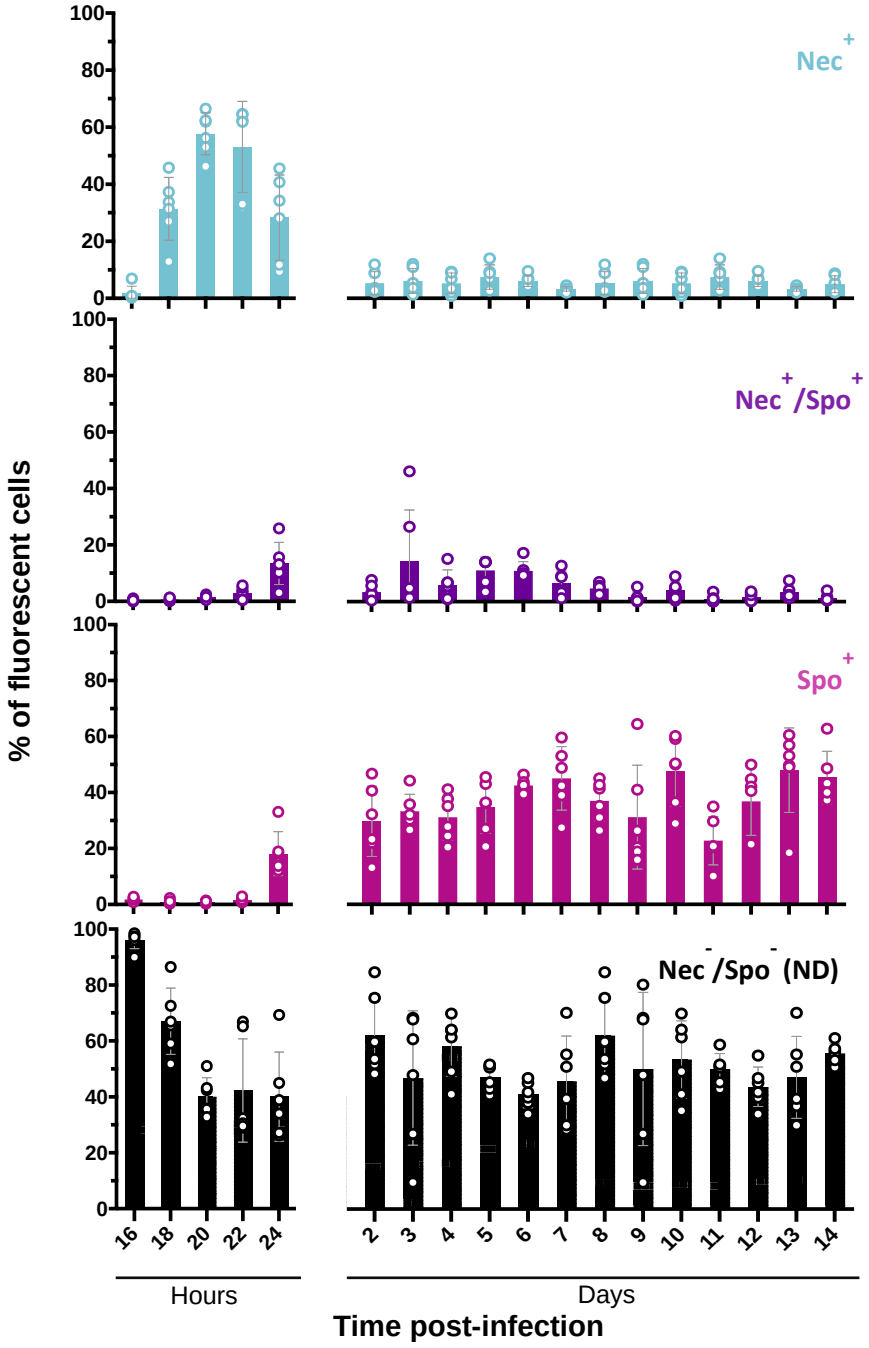
% of fluorescent cells
Nec+
Nec+/Spo+
Spo+
Nec-/Spo- (ND)
100
80
60
40
20
0
16
18
20
22
24
2
3
4
5
6
7
8
9
10
11
12
13
14
Hours
Days
Time post-infection

Figure 3

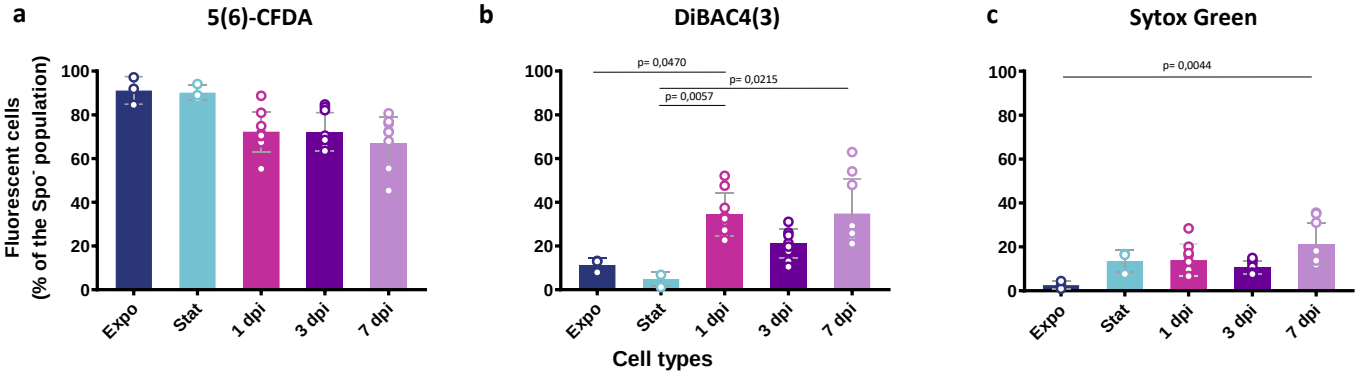
a
5(6)-CFDA
Fluorescent cells
(% of the Spo˙ population)
100
80
60
40
20
0
Expo
Stat
1 dpi
3 dpi
7 dpi
b
DiBAC4(3)
p= 0,0470
p= 0,0215
p= 0,0057
Cell types
c
Sytox Green
p= 0,0044

Figure 4

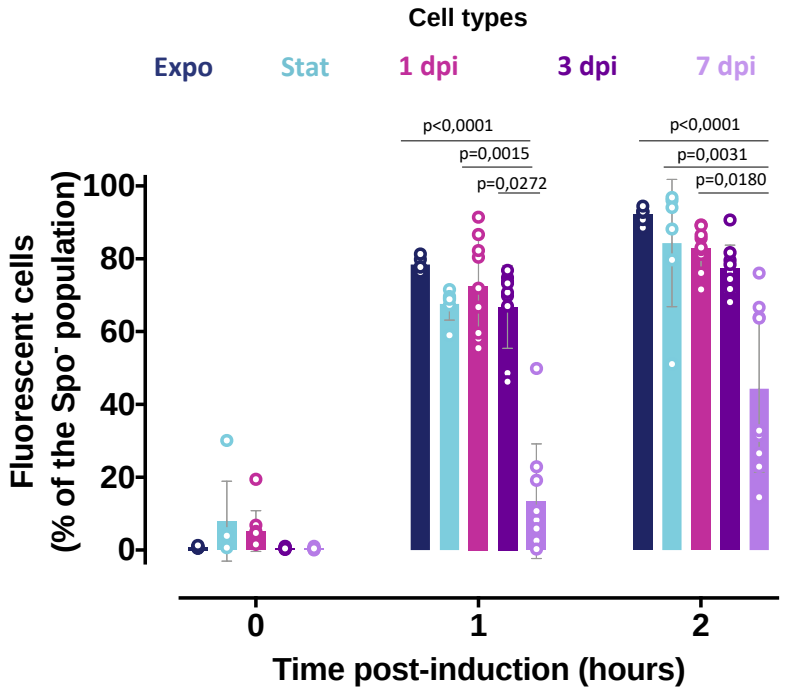
Cell types
Expo
Stat
1 dpi
3 dpi
7 dpi
p<0,0001
p=0,0015
p=0,0272
p<0,0001
p=0,0031
p=0,0180
Fluorescent cells
(% of the Spo⁻ population)
100
80
60
40
20
0
0
1
2
Time post-induction (hours)

Figure 5

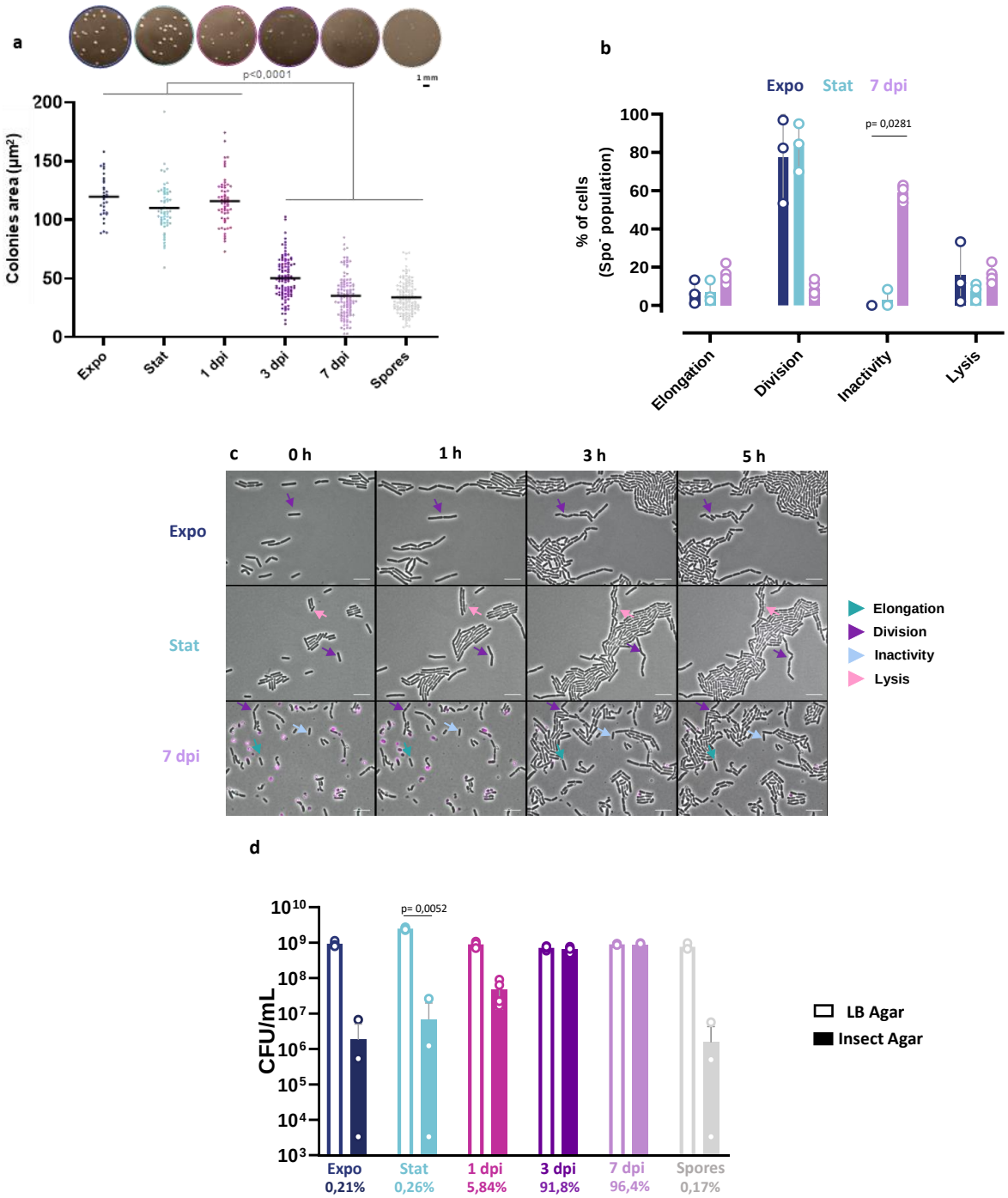
a
p<0,0001
1 mm
Colonies area (µm²)
200
150
100
50
0
Expo
Stat
1 dpi
3 dpi
7 dpi
Spores
b
Expo
Stat
7 dpi
p= 0,0281
% of cells
(Spo⁻ population)
100
80
60
40
20
0
Elongation
Division
Inactivity
Lysis
c
0 h
1 h
3 h
5 h
Expo
Stat
7 dpi
Elongation
Division
Inactivity
Lysis
d
p= 0,0052
CFU/mL
10¹⁰
10⁹
10⁸
10⁷
10⁶
10⁵
10⁴
10³
Expo
0,21%
Stat
0,26%
1 dpi
5,84%
3 dpi
91,8%
7 dpi
96,4%
Spores
0,17%
LB Agar
Insect Agar

Figure 6

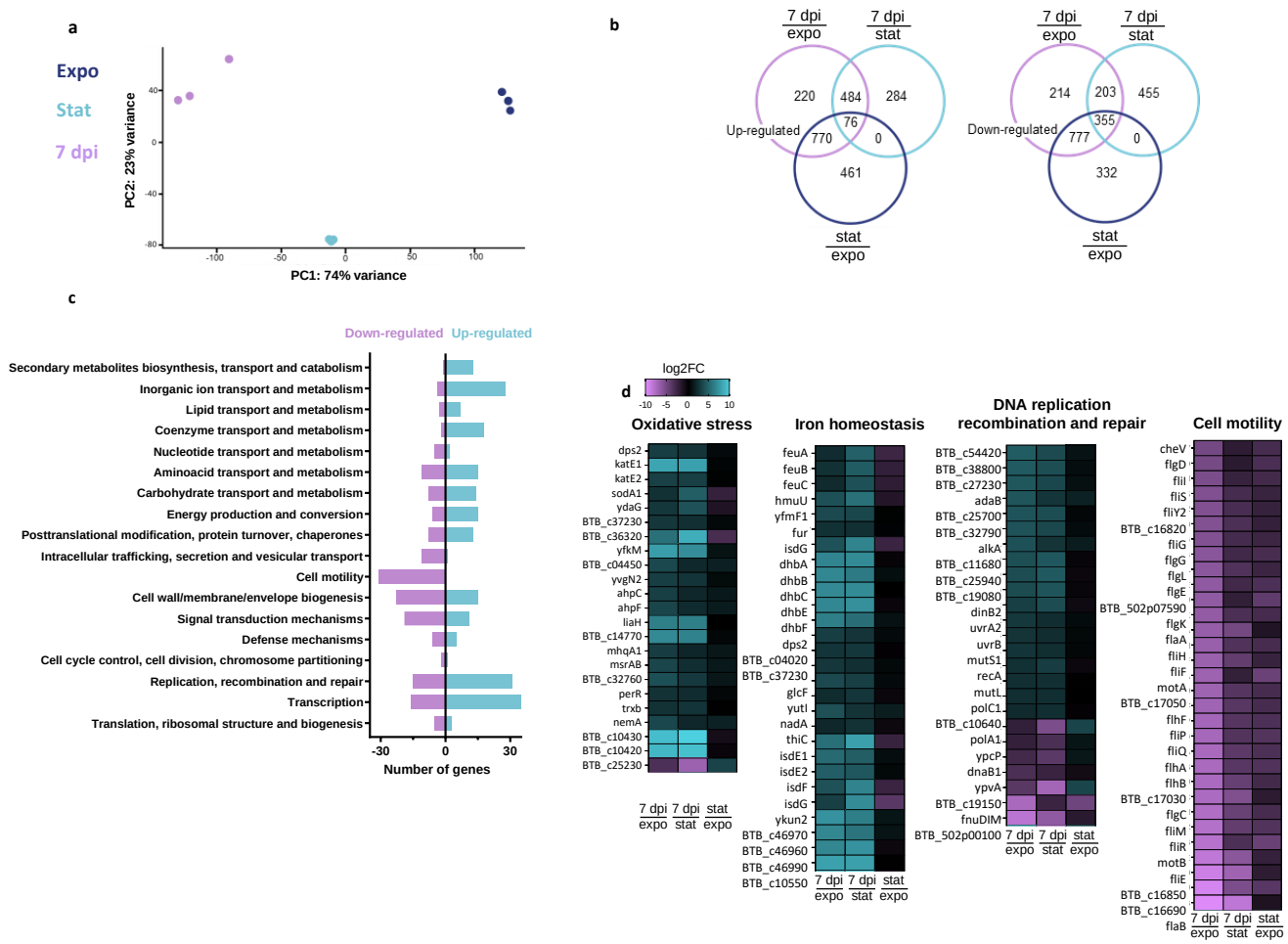
a
Expo
Stat
7 dpi
PC2: 23% variance
PC1: 74% variance
b
7 dpi expo
7 dpi stat
stat expo
Up-regulated
220
484
284
76
770
0
461
Down-regulated
214
203
455
355
777
0
332
c
Down-regulated
Up-regulated
Secondary metabolites biosynthesis, transport and catabolism
Inorganic ion transport and metabolism
Lipid transport and metabolism
Coenzyme transport and metabolism
Nucleotide transport and metabolism
Aminoacid transport and metabolism
Carbohydrate transport and metabolism
Energy production and conversion
Posttranslational modification, protein turnover, chaperones
Intracellular trafficking, secretion and vesicular transport
Cell motility
Cell wall/membrane/envelope biogenesis
Signal transduction mechanisms
Defense mechanisms
Cell cycle control, cell division, chromosome partitioning
Replication, recombination and repair
Transcription
Translation, ribosomal structure and biogenesis
Number of genes
d
log2FC
Oxidative stress
Iron homeostasis
DNA replication recombination and repair
Cell motility
7 dpi expo
7 dpi stat
stat expo

Figure 7

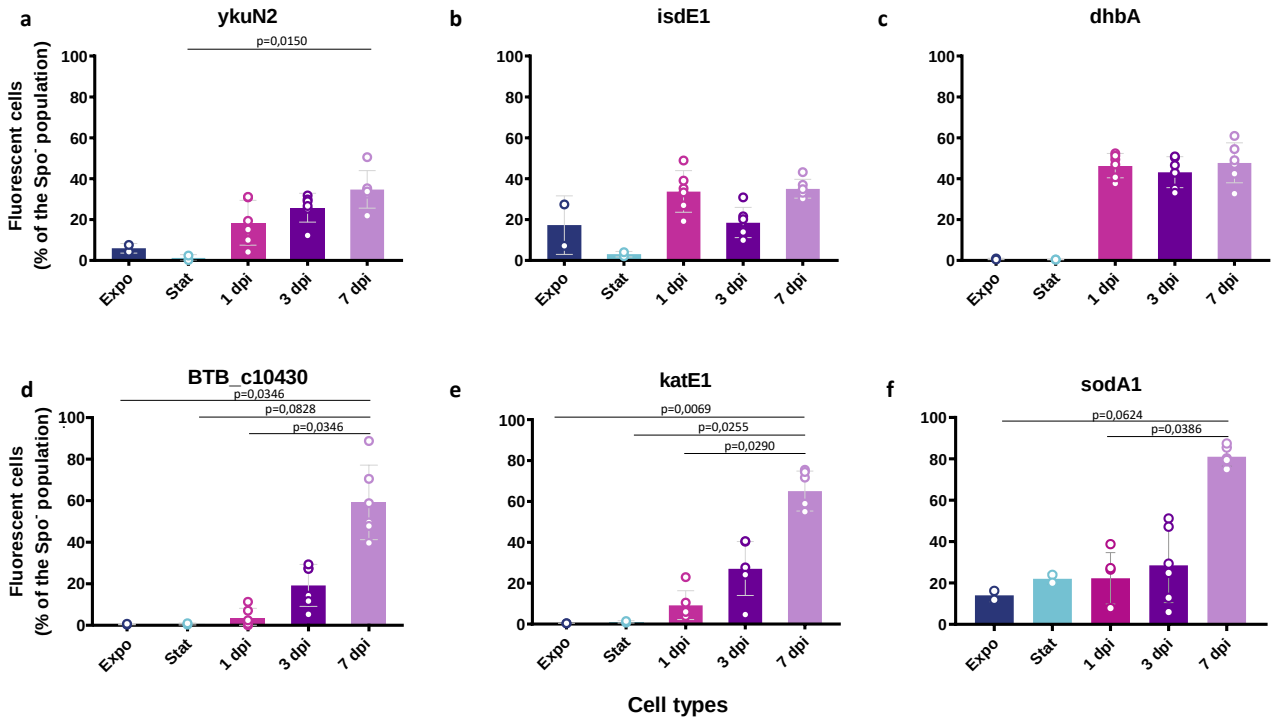
a
ykuN2
p=0,0150
b
isdE1
c
dhbA
d
BTB_c10430
p=0,0346
p=0,0828
p=0,0346
e
katE1
p=0,0069
p=0,0255
p=0,0290
f
sodA1
p=0,0624
p=0,0386
Fluorescent cells
(% of the Spo⁻ population)
0
20
40
60
80
100
Expo
Stat
1 dpi
3 dpi
7 dpi
Cell types